

Received 15 June 2022
Accepted 22 June 2022

Edited by L. Van Meervelt, Katholieke Universiteit Leuven, Belgium

Keywords: crystal structure; 1,6-dihydropyridine; hydrogen bond; C—Br···π interactions; Hirshfeld surface analysis.

CCDC reference: 2181245

Supporting information: this article has supporting information at journals.iucr.org/e

Crystal structure and Hirshfeld surface analysis of 2-(4-bromophenyl)-4-methyl-6-oxo-1-phenyl-1,6-dihydropyridine-3-carbonitrile

Farid N. Naghiyev,^a Victor N. Khrustalev,^{b,c} Ekaterina V. Dobrokhotova,^c Mehmet Akkurt,^d Ali N. Khalilov,^{e,a} Ajaya Bhattacharai^{f*} and Ibrahim G. Mamedov^a

^aDepartment of Chemistry, Baku State University, Z. Khalilov str. 23, Az, 1148, Baku, Azerbaijan, ^bPeoples' Friendship University of Russia (RUDN University), Miklukho-Maklay St., 6, Moscow, 117198, Russian Federation, ^cN. D. Zelinsky Institute of Organic Chemistry RAS, Leninsky Prospekt 47, Moscow, 119991, Russian Federation, ^dDepartment of Physics, Faculty of Sciences, Erciyes University, 38039 Kayseri, Turkey, ^e"Composite Materials" Scientific Research Center, Azerbaijan State Economic University (UNEC), H. Aliyev str. 135, Az 1063, Baku, Azerbaijan, and ^fDepartment of Chemistry, M.M.A.M.C (Tribhuvan University) Biratnagar, Nepal. *Correspondence e-mail: ajaya.bhattacharai@mmamc.tu.edu.np

In the title compound, $C_{19}H_{13}BrN_2O$, the pyridine ring is essentially planar [maximum deviation = 0.024 (4) Å for the N atom] and makes dihedral angles of 74.6 (2) and 65.8 (2)°, respectively, with the phenyl and bromophenyl rings, which subtend a dihedral angle of 63.1 (2)°. In the crystal, molecules are connected along the *c*-axis direction via C—Br···π interactions, generating zigzag chains parallel to the (010) plane. C—H···N and C—H···O hydrogen-bonding interactions further connect the molecules, forming a three-dimensional network and reinforcing the molecular packing. Hirshfeld surface analysis indicates that the most important contributions to the crystal packing are from H···H (36.2%), C···H/H···C (21.6%), N···H/H···N (12.2%), and Br···H/H···Br (10.8%) interactions.

1. Chemical context

C—C and C—N bond-forming reactions are a cornerstone of organic synthesis, materials science and medicinal chemistry (Zubkov *et al.*, 2018; Shikhaliyev *et al.*, 2019; Viswanathan *et al.*, 2019; Gurbanov *et al.*, 2020). Nitrogen heterocycles, particularly those including the 2-pyridone core, play a key role in medicinal chemistry and natural product synthesis (Sośnicki & Idzik, 2019; Duruskari *et al.*, 2020; Sangwan *et al.*, 2022). We report herein the synthesis of 2-pyridone, **2**, on the basis of a one-step reaction of acetoacetanilide with 3-(4-bromophenyl)-3-oxopropanenitrile (Path **B**). Under two-step reaction conditions (Fig. 1), the interaction of acetoacetanilide with 3-oxo-3-phenylpropanenitrile led to the formation of another 2-pyridone, **1** (Path **A**), reported in the literature (Wardakhan & Agami, 2001).

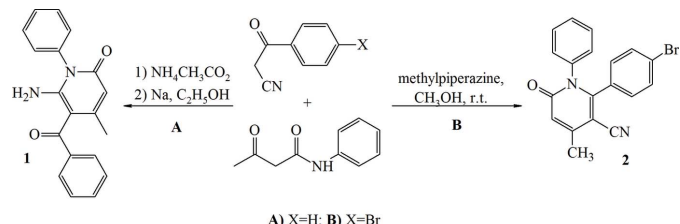
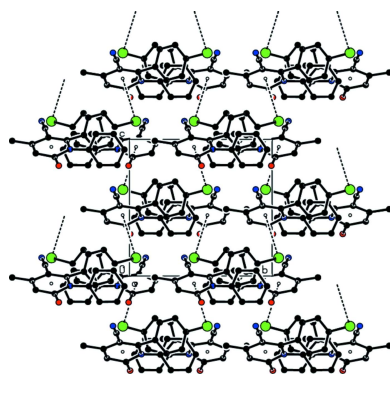
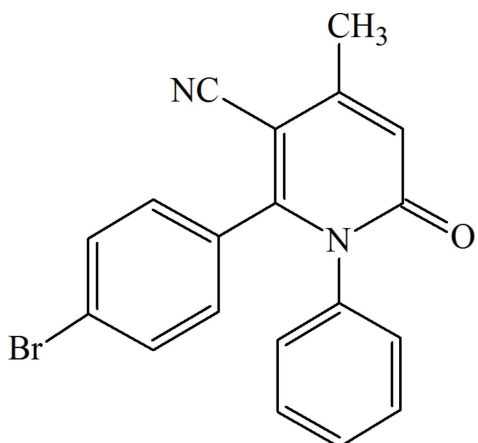


Figure 1

The reaction of acetoacetanilide with 3-oxo-3-arylpalanenitriles.



Thus, in the framework of our ongoing structural studies (Naghiyev *et al.*, 2020, 2021, 2022; Khalilov *et al.*, 2022), we report the crystal structure and Hirshfeld surface analysis of the title compound, 2-(4-bromophenyl)-4-methyl-6-oxo-1-phenyl-1,6-dihdropyridine-3-carbonitrile.

2. Structural commentary

In the title compound, (Fig. 2), the pyridine ring (N1/C2–C6) is largely planar [maximum deviation = 0.024 (4) Å for N1]. The phenyl and bromophenyl groups are linked to the central pyridine ring in an equatorial arrangement. The pyridine ring subtends dihedral angles of 74.6 (2) and 65.8 (2)° with the phenyl (C7–C12) and bromophenyl (C15–C20) rings, which in turn make a dihedral angle of 63.1 (2)° with each other.

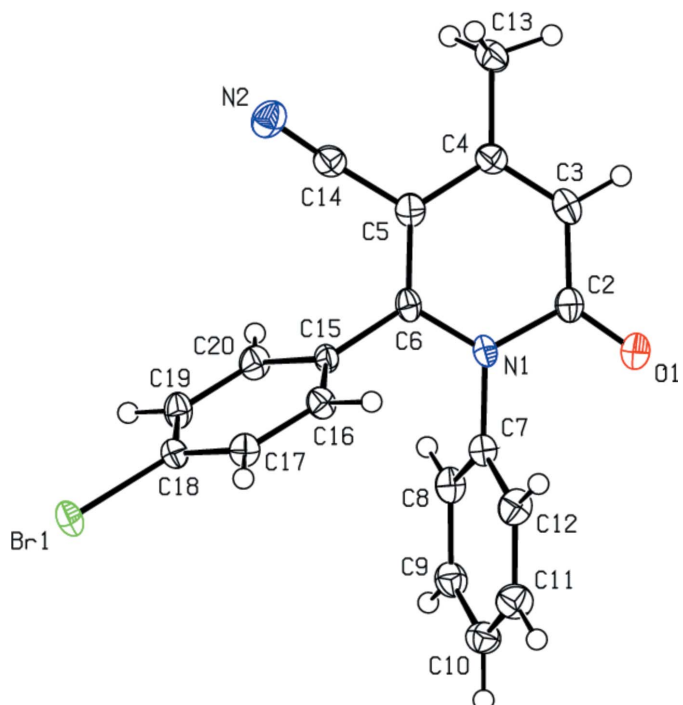


Figure 2

The molecular structure of the title compound. Displacement ellipsoids are drawn at the 50% probability level.

Table 1
Hydrogen-bond geometry (\AA , $^\circ$).

$D - \text{H} \cdots A$	$D - \text{H}$	$\text{H} \cdots A$	$D \cdots A$	$D - \text{H} \cdots A$
C16—H16···N2 ⁱ	0.95	2.55	3.234 (6)	129
C17—H17···O1 ⁱⁱ	0.95	2.56	3.342 (6)	140
C20—H20···O1 ⁱⁱⁱ	0.95	2.40	3.256 (6)	150

$$\begin{array}{lll} \text{Symmetry} & \text{codes:} & \\ \text{---} & \text{(i)} & -x + \frac{3}{2}, y - \frac{1}{2}, z - \frac{1}{2}; \\ -x + 1, -y + 1, z + \frac{1}{2}. & \text{(ii)} & x + \frac{1}{2}, -y + \frac{1}{2}, z; \\ & \text{(iii)} & \end{array}$$

3. Supramolecular features and Hirshfeld surface analysis

Fig. 3 shows a general view of the C—H···N and C—H···O hydrogen bonds (Table 1) and C—Br···π interactions in the unit cell of the title compound. In the crystal, molecules are joined along the *c*-axis direction by C—Br···π interactions [C18—Br1···Cg1^{iv}: C18—Br1 = 1.944 (4) Å, Br1···Cg1^{iv} = 3.4788 (18) Å, C18···Cg1^{iv} = 4.283 (5) Å, C18—Br1···Cg1^{iv} = 100.50 (13)°; Cg1 is the centroid of the N1/C2—C6 pyridine ring; symmetry code: (iv) $x + \frac{3}{2}, -y - \frac{1}{2}, z$], generating zigzag chains parallel to the (010) plane (Figs. 4 and 5). C—H···N and C—H···O hydrogen bonds link these molecules, establishing a three-dimensional network and strengthening the molecular packing.

*CrystalExplorer*17.5 (Turner *et al.*, 2017) was used to analyse and visualize the intermolecular interactions of the title compound. Fig. 6*a,b* depicts the front and back sides of the Hirshfeld surface plotted over d_{norm} in the range of -0.2437 to 1.2589 a.u. The red spots on the Hirshfeld surface indicate C—H \cdots N and C—H \cdots O interactions (Table 1).

The overall two-dimensional fingerprint plot for the title compound and those delineated into H···H (36.2%, Fig. 7b), C···H/H···C (21.6%, Fig. 7c), N···H/H···N (12.2%, Fig. 7d), and Br···H/H···Br (10.8%, Fig. 7e) interactions, as well as

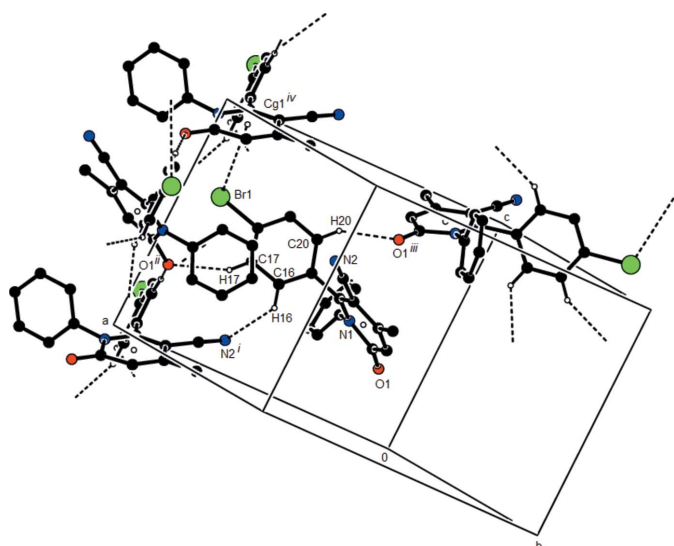
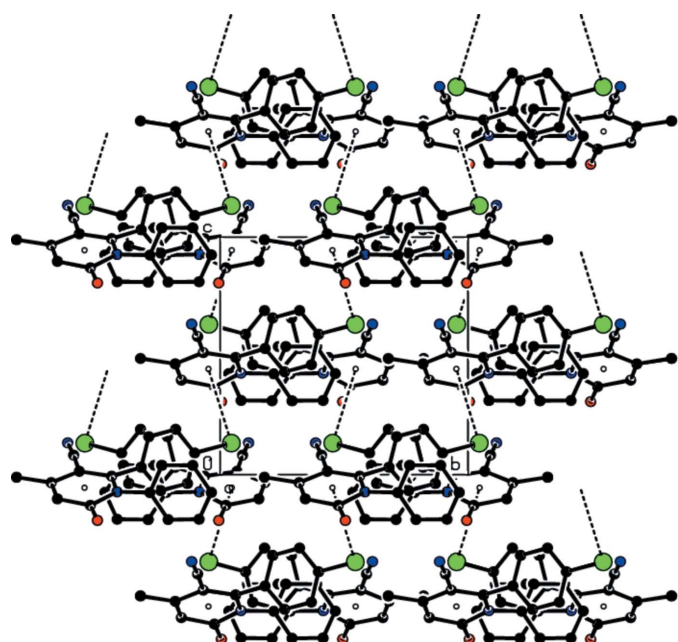


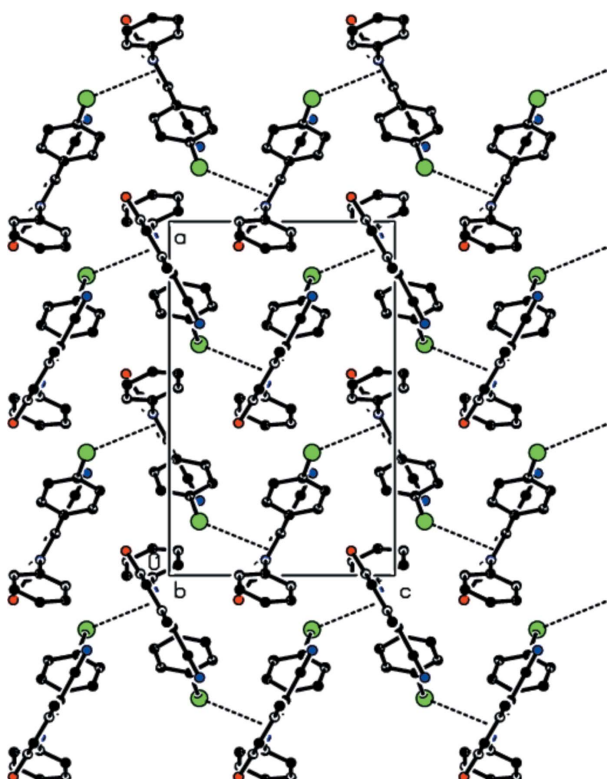
Figure 3

A general view of the C—H···N, C—H···O hydrogen bonds and C—Br···π interactions of the title compound. Symmetry codes: (i) $x + \frac{3}{2}$, $-y - \frac{1}{2}$, $z - 1$; (ii) $-x + \frac{1}{2}$, $y + \frac{1}{2}$, $z + \frac{1}{2}$; (iii) $-x + 1$, $-y + 1$, $z + \frac{1}{2}$; (iv) $\frac{3}{2} - x$, $-\frac{1}{2} + y$, $\frac{1}{2} + z$.

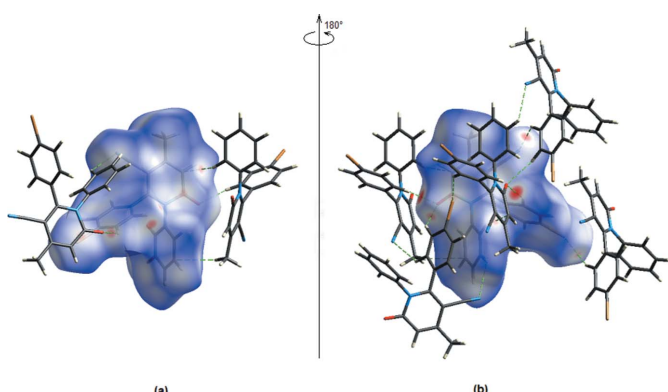
**Figure 4**

Packing view of the title compound along the *a* axis showing the C–Br··· π interactions as dashed lines.

their relative contributions to the Hirshfeld surface, are shown in Fig. 7, while Tables 1 and 2 provide data on the distinct intermolecular contacts. The remaining weak interactions (contribution percentages) are O···H/H···O (7.2%), Br···C/

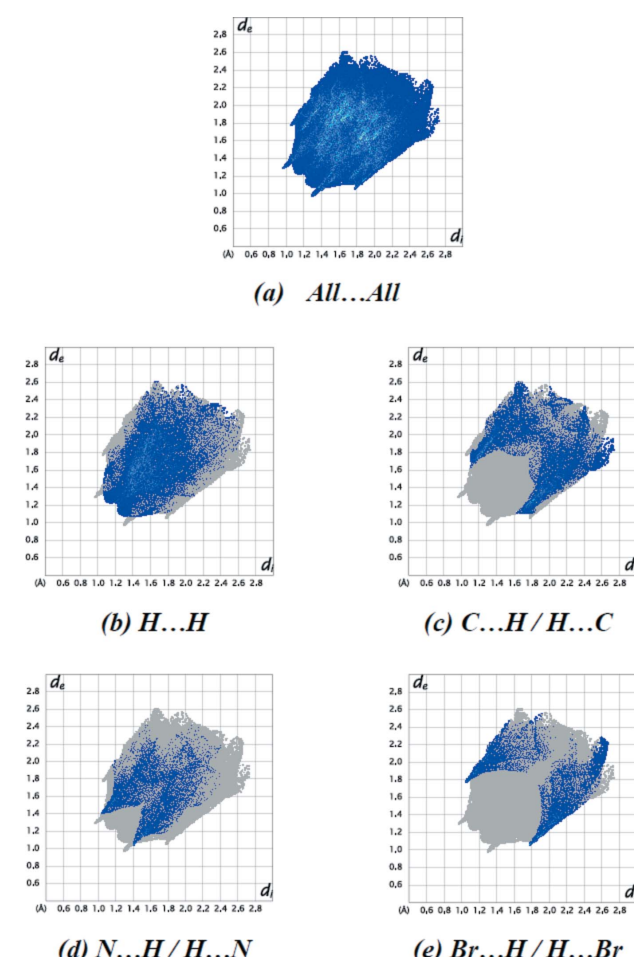
**Figure 5**

Packing view of the title compound along the *b* axis with the C–Br··· π interactions indicated by dashed lines.

**Figure 6**

(*a*) Front and (*b*) back sides of the three-dimensional Hirshfeld surface of the title compound mapped over d_{norm} , with a fixed colour scale of –0.2437 to 1.2589 a.u.

C···Br (3.6%), C···C (3.0%), Br·N/N···Br (2.2%), O···C/C···O (2.2%) and Br···O/O···Br (0.8%), these contacts having little directional influence on the packing.

**Figure 7**

The two-dimensional fingerprint plots of the title compound, showing (*a*) all interactions, and delineated into (*b*) H···H, (*c*) C···H/H···C, (*d*) N···H/H···N and (*e*) Br···H/H···Br interactions. [d_e and d_i represent the distances from a point on the Hirshfeld surface to the nearest atoms outside (external) and inside (internal) the surface, respectively].

Table 2Summary of short interatomic contacts (\AA) in the title compound.

Contact	Distance	Symmetry operation
H19 \cdots H13B	2.59	$\frac{3}{2} - x, -\frac{1}{2} + y, \frac{1}{2} + z$
H17 \cdots O1	2.56	$\frac{1}{2} + x, \frac{1}{2} - y, z$
O1 \cdots H20	2.40	$1 - x, 1 - y, -\frac{1}{2} + z$
N2 \cdots H16	2.55	$\frac{3}{2} - x, \frac{1}{2} + y, \frac{1}{2} + z$
C9 \cdots H11	2.99	$1 - x, -y, \frac{1}{2} + z$
C10 \cdots H13A	3.03	$x, -1 + y, z$

4. Database survey

A search of the Cambridge Structural Database (CSD version 5.42, updated September 2021; Groom *et al.*, 2016) for the basic skeleton of 6-oxo-1,6-dihdropyridine gave five compounds very similar to the title compound.

The cations in the crystal of FONDOC01 (Pérez-Aguirre *et al.*, 2015) interact with the anions through O \cdots H \cdots O and N \cdots H \cdots O hydrogen bonds, forming a three-dimensional supramolecular network.

In the crystal of SECPUN (Thanigaimani *et al.*, 2012), an N \cdots H \cdots O hydrogen bond connects the cation and anion, while a pair of N \cdots H \cdots O hydrogen bonds connects the two anions with an $R_2^2(8)$ ring motif. Weak N \cdots H \cdots O and C \cdots H \cdots O hydrogen bonds connect the aggregates, forming a three-dimensional network.

The ion pairs in the crystal of SUYXIU (Hemamalini & Fun, 2010) are linked by O \cdots H \cdots O, N \cdots H \cdots O, N \cdots H \cdots Br and C \cdots H \cdots O hydrogen bonds, producing a two-dimensional network parallel to the *bc* plane.

In the crystal of XOZCUL (Shishkina *et al.*, 2009), the pyridine-3-carboxylate molecules form layers parallel to (010), which are linked by hydrogen bonds mediated by the bridging solvate molecules.

The asymmetric unit of GIHCOQ (Gupta *et al.*, 2007) contains four molecules. The compound forms hydrogen-bonded sheets parallel to the [001] direction *via* intermolecular N \cdots H \cdots O and O \cdots H \cdots O hydrogen bonds. Each sheet is made up of linked dimers generated by $R_2^2(8)$ N \cdots H \cdots O hydrogen-bonded motifs. Intermolecular N \cdots H \cdots O and O \cdots H \cdots O hydrogen bonds generate sheets parallel to the [001] direction. Each sheet is made up of linked dimers formed by N \cdots H \cdots O hydrogen bonds with $R_2^2(8)$ motifs.

5. Synthesis and crystallization

To a solution of 3-(4-bromophenyl)-3-oxopropanenitrile (1.14 g; 5.1 mmol) and acetoacetanilide (0.92 g; 5.2 mmol) in methanol (25 mL), methylpyperazine (3 drops) was added and the mixture was stirred at room temperature for 48 h. Then 15 mL of methanol were removed from the reaction mixture, which was left overnight. The precipitated crystals were separated by filtration and recrystallized from ethanol/water (1:1) solution (yield 49%; m.p. 484–485 K).

^1H NMR (300 MHz, DMSO-*d*₆, ppm): 2.21 (*s*, 3H, CH₃); 6.61 (*s*, 1H, ==CH); 7.19–7.89 (*m*, 9H, 9Ar–H). ^{13}C NMR (75 MHz, DMSO-*d*₆, ppm): 20.58 (CH₃), 94.75 (==C_{quat}).

Table 3
Experimental details.

Crystal data	
Chemical formula	C ₁₉ H ₁₃ BrN ₂ O
<i>M</i> _r	365.21
Crystal system, space group	Orthorhombic, <i>Pna2</i> ₁
Temperature (K)	100
<i>a</i> , <i>b</i> , <i>c</i> (\AA)	15.58979 (16), 10.33883 (10), 9.91195 (9)
<i>V</i> (\AA^3)	1597.61 (3)
<i>Z</i>	4
Radiation type	Cu $K\alpha$
μ (mm^{-1})	3.55
Crystal size (mm)	0.25 \times 0.24 \times 0.21
Data collection	
Diffractometer	XtaLAB Synergy, Dualflex, HyPix
Absorption correction	Multi-scan (<i>CrysAlis PRO</i> ; Rigaku OD, 2021)
<i>T</i> _{min} , <i>T</i> _{max}	0.413, 0.462
No. of measured, independent and observed [$I > 2\sigma(I)$] reflections	45325, 3359, 3339
<i>R</i> _{int}	0.047
(sin θ/λ) _{max} (\AA^{-1})	0.648
Refinement	
$R[F^2 > 2\sigma(F^2)]$, <i>wR</i> (F^2), <i>S</i>	0.037, 0.099, 1.05
No. of reflections	3359
No. of parameters	209
No. of restraints	1
H-atom treatment	H-atom parameters constrained
$\Delta\rho_{\text{max}}$, $\Delta\rho_{\text{min}}$ (e \AA^{-3})	1.27, -0.89
Absolute structure	Flack <i>x</i> determined using 1531 quotients [(I ⁺) $-(I^-)$]/[(I ⁺) $+(I^-)$] (Parsons <i>et al.</i> , 2013).
Absolute structure parameter	-0.012 (18)

Computer programs: *CrysAlis PRO* (Rigaku OD, 2021), *SHELXT* (Sheldrick, 2015a), *SHELXL* (Sheldrick, 2015b), *ORTEP-3 for Windows* (Farrugia, 2012) and *PLATON* (Spek, 2020).

116.17 (CN), 118.27 (==CH), 120.87 (2CH_{arom}), 122.95 (Br—C_{arom}), 125.30 (CH_{arom}), 127.43 (Carom), 129.55 (2CH_{arom}), 129.70 (2CH_{arom}), 134.09 (2CH_{arom}), 138.94 (Carom), 143.81 (==C_{quat}), 153.68 (==C_{quat}—N), 165.44 (C=O).

6. Refinement

Crystal data, data collection and structure refinement details are summarized in Table 3. All C-bound H atoms were placed at calculated positions and refined using a riding model, with C—H = 0.95 \AA for aromatic H atoms and 0.98 \AA for methyl H atoms, and with *U*_{iso}(H) = 1.2 or 1.5*U*_{eq}(C). Owing to poor agreement between observed and calculated intensities, nineteen outliers (8 4 0, 17 6 2, 13 9 2, 18 5 0, 9 11 2, 18 2 5, 17 3 6, 0 12 4, 4 11 1, 3 5 0, 18 5 2, 2 0 1, 5 3 2, 18 2 5, 15 8 2, 0 10 8, 5 3 2, 0 12 4 and 17 6 1) were omitted in the final cycles of refinement.

Acknowledgements

Author contributions are as follows. Conceptualization, ANK and IGM; methodology, ANK and IGM; investigation, FNN, ANK, MA and EVD; writing (original draft), MA and ANK; writing (review and editing of the manuscript), MA and ANK; visualization, MA, ANK and IGM; funding acquisition, VNK,

AB and ANK; resources, AB, VNK and EVD; supervision, ANK and MA.

Funding information

This study was supported by Baku State University and the Ministry of Science and Higher Education of the Russian Federation [award No. 075–03–2020-223 (FSSF-2020-0017)].

References

- Duruskari, G. S., Asgarova, A. R., Aliyeva, K. N., Musayeva, S. A. & Maharramov, A. M. (2020). *Russ. J. Org. Chem.* **56**, 712–715.
- Farrugia, L. J. (2012). *J. Appl. Cryst.* **45**, 849–854.
- Groom, C. R., Bruno, I. J., Lightfoot, M. P. & Ward, S. C. (2016). *Acta Cryst. B* **72**, 171–179.
- Gupta, S., Long, S. & Li, T. (2007). *Acta Cryst. E* **63**, o2784.
- Gurbanov, A. V., Kuznetsov, M. L., Demukhamedova, S. D., Alieva, I. N., Godjaev, N. M., Zubkov, F. I., Mahmudov, K. T. & Pombeiro, A. J. L. (2020). *CrystEngComm*, **22**, 628–633.
- Hemamalini, M. & Fun, H.-K. (2010). *Acta Cryst. E* **66**, o2246–o2247.
- Khalilov, A. N., Khrustalev, V. N., Tereshina, T. A., Akkurt, M., Rzayev, R. M., Akobirshoeva, A. A. & Mamedov, İ. G. (2022). *Acta Cryst. E* **78**, 525–529.
- Naghiyev, F. N., Akkurt, M., Askerov, R. K., Mamedov, I. G., Rzayev, R. M., Chyrka, T. & Maharramov, A. M. (2020). *Acta Cryst. E* **76**, 720–723.
- Naghiyev, F. N., Khrustalev, V. N., Novikov, A. P., Akkurt, M., Rzayev, R. M., Akobirshoeva, A. A. & Mamedov, İ. G. (2022). *Acta Cryst. E* **78**, 554–558.
- Naghiyev, F. N., Tereshina, T. A., Khrustalev, V. N., Akkurt, M., Rzayev, R. M., Akobirshoeva, A. A. & Mamedov, İ. G. (2021). *Acta Cryst. E* **77**, 516–521.
- Parsons, S., Flack, H. D. & Wagner, T. (2013). *Acta Cryst. B* **69**, 249–259.
- Pérez-Aguirre, R., Pérez-Yáñez, S., Beobide, G., Castillo, O., Gutiérrez-Zorrilla, J. M. & Luque, A. (2015). *Acta Cryst. E* **71**, m238–m239.
- Rigaku OD (2021). *CrysAlis PRO*. Rigaku Oxford Diffraction, Tokyo, Japan.
- Sangwan, S., Yadav, N., Kumar, R., Chauhan, S., Dhanda, V., Walia, P. & Duhan, A. (2022). *Eur. J. Med. Chem.* **232**, 114199.
- Sheldrick, G. M. (2015a). *Acta Cryst. A* **71**, 3–8.
- Sheldrick, G. M. (2015b). *Acta Cryst. C* **71**, 3–8.
- Shikaliyev, N. Q., Kuznetsov, M. L., Maharramov, A. M., Gurbanov, A. V., Ahmadova, N. E., Nenajdenko, V. G., Mahmudov, K. T. & Pombeiro, A. J. L. (2019). *CrystEngComm*, **21**, 5032–5038.
- Shishkina, S. V., Shishkin, O. V., Ukrainets, I. V., Tkach, A. A. & Grinevich, L. A. (2009). *Acta Cryst. E* **65**, o1984.
- Sośnicki, J. G. & Idzik, T. J. (2019). *Synthesis*, **51**, 3369–3396.
- Spek, A. L. (2020). *Acta Cryst. E* **76**, 1–11.
- Thanigaimani, K., Farhadikoutenaei, A., Khalib, N. C., Arshad, S. & Razak, I. A. (2012). *Acta Cryst. E* **68**, o3151–o3152.
- Turner, M. J., McKinnon, J. J., Wolff, S. K., Grimwood, D. J., Spackman, P. R., Jayatilaka, D. & Spackman, M. A. (2017). *CrystalExplorer17*. University of Western Australia. <http://Hirshfeldsurface.net>
- Viswanathan, A., Kute, D., Musa, A., Konda Mani, S., Sipilä, V., Emmert-Streib, F., Zubkov, F. I., Gurbanov, A. V., Yli-Harja, O. & Kandhavelu, M. (2019). *Eur. J. Med. Chem.* **166**, 291–303.
- Wardakhan, W. W. & Agami, S. M. (2001). *Egypt. J. Chem.* **44**, 315–333.
- Zubkov, F. I., Mertsalov, D. F., Zaytsev, V. P., Varlamov, A. V., Gurbanov, A. V., Dorovatovskii, P. V., Timofeeva, T. V., Khrustalev, V. N. & Mahmudov, K. T. (2018). *J. Mol. Liq.* **249**, 949–952.

supporting information

Acta Cryst. (2022). E78, 761–765 [https://doi.org/10.1107/S2056989022006466]

Crystal structure and Hirshfeld surface analysis of 2-(4-bromophenyl)-4-methyl-6-oxo-1-phenyl-1,6-dihdropyridine-3-carbonitrile

Farid N. Naghiyev, Victor N. Khrustalev, Ekaterina V. Dobrokhotova, Mehmet Akkurt, Ali N. Khalilov, Ajaya Bhattacharai and İbrahim G. Mamedov

Computing details

Data collection: *CrysAlis PRO* (Rigaku OD, 2021); cell refinement: *CrysAlis PRO* (Rigaku OD, 2021); data reduction: *CrysAlis PRO* (Rigaku OD, 2021); program(s) used to solve structure: *SHELXT* (Sheldrick, 2015a); program(s) used to refine structure: *SHELXL* (Sheldrick, 2015b); molecular graphics: *ORTEP-3 for Windows* (Farrugia, 2012); software used to prepare material for publication: *PLATON* (Spek, 2020).

2-(4-Bromophenyl)-4-methyl-6-oxo-1-phenyl-1,6-dihdropyridine-3-carbonitrile

Crystal data



$M_r = 365.21$

Orthorhombic, $Pna2_1$

$a = 15.58979$ (16) Å

$b = 10.33883$ (10) Å

$c = 9.91195$ (9) Å

$V = 1597.61$ (3) Å³

$Z = 4$

$F(000) = 736$

$D_x = 1.518 \text{ Mg m}^{-3}$

$\text{Cu } K\alpha$ radiation, $\lambda = 1.54178$ Å

Cell parameters from 35934 reflections

$\theta = 2.7\text{--}79.0^\circ$

$\mu = 3.55 \text{ mm}^{-1}$

$T = 100$ K

Prism, colourless

0.25 × 0.24 × 0.21 mm

Data collection

XtaLAB Synergy, Dualflex, HyPix

diffractometer

Radiation source: micro-focus sealed X-ray tube

φ and ω scans

Absorption correction: multi-scan
(CrysAlisPro; Rigaku OD, 2021)

$T_{\min} = 0.413$, $T_{\max} = 0.462$

45325 measured reflections

3359 independent reflections

3339 reflections with $I > 2\sigma(I)$

$R_{\text{int}} = 0.047$

$\theta_{\max} = 88.3^\circ$, $\theta_{\min} = 5.1^\circ$

$h = -19\text{--}19$

$k = -12\text{--}12$

$l = -12\text{--}12$

Refinement

Refinement on F^2

Least-squares matrix: full

$R[F^2 > 2\sigma(F^2)] = 0.037$

$wR(F^2) = 0.099$

$S = 1.05$

3359 reflections

209 parameters

1 restraint

Primary atom site location: difference Fourier map

Secondary atom site location: difference Fourier map

Hydrogen site location: inferred from neighbouring sites

H-atom parameters constrained

$w = 1/[\sigma^2(F_{\text{o}}^2) + (0.0658P)^2 + 1.8045P]$
where $P = (F_{\text{o}}^2 + 2F_{\text{c}}^2)/3$

$(\Delta/\sigma)_{\max} < 0.001$
 $\Delta\rho_{\max} = 1.27 \text{ e \AA}^{-3}$
 $\Delta\rho_{\min} = -0.89 \text{ e \AA}^{-3}$

Absolute structure: Flack x determined using
 1531 quotients $[(I^{\prime})-(I)]/[(I^{\prime})+(I)]$ (Parsons *et al.*, 2013).
 Absolute structure parameter: $-0.012 (18)$

Special details

Experimental. CrysAlisPro 1.171.41.117a (Rigaku OD, 2021) Empirical absorption correction using spherical harmonics, implemented in SCALE3 ABSPACK scaling algorithm.

Geometry. All esds (except the esd in the dihedral angle between two l.s. planes) are estimated using the full covariance matrix. The cell esds are taken into account individually in the estimation of esds in distances, angles and torsion angles; correlations between esds in cell parameters are only used when they are defined by crystal symmetry. An approximate (isotropic) treatment of cell esds is used for estimating esds involving l.s. planes.

Fractional atomic coordinates and isotropic or equivalent isotropic displacement parameters (\AA^2)

	x	y	z	$U_{\text{iso}}^*/U_{\text{eq}}$
Br1	0.84710 (3)	-0.04550 (4)	0.63282 (7)	0.02494 (16)
O1	0.4307 (2)	0.4948 (4)	0.3074 (4)	0.0278 (7)
N1	0.5437 (2)	0.4161 (4)	0.4275 (4)	0.0188 (7)
N2	0.7885 (2)	0.6147 (4)	0.6339 (5)	0.0294 (7)
C2	0.4948 (3)	0.5231 (5)	0.3709 (4)	0.0216 (10)
C3	0.5263 (3)	0.6562 (5)	0.3980 (4)	0.0238 (9)
H3	0.4934	0.7271	0.3657	0.029*
C4	0.5993 (3)	0.6812 (4)	0.4665 (4)	0.0215 (8)
C5	0.6468 (3)	0.5678 (5)	0.5140 (5)	0.0222 (10)
C6	0.6185 (3)	0.4373 (4)	0.4937 (4)	0.0188 (8)
C7	0.5051 (3)	0.2830 (4)	0.4247 (4)	0.0205 (8)
C8	0.4705 (3)	0.2349 (5)	0.5395 (5)	0.0237 (9)
H8	0.4733	0.2837	0.6205	0.028*
C9	0.4295 (3)	0.1103 (5)	0.5393 (5)	0.0263 (9)
H9	0.4052	0.0789	0.6209	0.032*
C10	0.4243 (3)	0.0354 (5)	0.4255 (5)	0.0268 (10)
H10	0.3970	-0.0467	0.4261	0.032*
C11	0.4602 (3)	0.0848 (5)	0.3123 (5)	0.0290 (10)
H11	0.4587	0.0354	0.2315	0.035*
C12	0.5005 (3)	0.2097 (5)	0.3110 (5)	0.0260 (9)
H12	0.5243	0.2417	0.2293	0.031*
C13	0.6315 (3)	0.8212 (5)	0.4893 (5)	0.0274 (10)
H13A	0.5887	0.8824	0.4551	0.041*
H13B	0.6857	0.8338	0.4412	0.041*
H13C	0.6403	0.8359	0.5859	0.041*
C14	0.7262 (3)	0.5907 (4)	0.5820 (5)	0.0233 (9)
C15	0.6711 (3)	0.3187 (4)	0.5311 (4)	0.0174 (8)
C16	0.7071 (3)	0.2397 (4)	0.4329 (4)	0.0201 (8)
H16	0.6956	0.2589	0.3409	0.024*
C17	0.7600 (3)	0.1318 (4)	0.4629 (4)	0.0214 (8)
H17	0.7843	0.0813	0.3924	0.026*
C18	0.7751 (3)	0.1027 (4)	0.5913 (4)	0.0205 (8)
C19	0.7397 (3)	0.1793 (5)	0.6909 (4)	0.0232 (9)

H19	0.7505	0.1587	0.7828	0.028*
C20	0.6878 (3)	0.2878 (4)	0.6599 (4)	0.0230 (9)
H20	0.6647	0.3389	0.7307	0.028*

Atomic displacement parameters (\AA^2)

	U^{11}	U^{22}	U^{33}	U^{12}	U^{13}	U^{23}
Br1	0.0283 (2)	0.0232 (3)	0.0233 (2)	0.00633 (14)	-0.0028 (2)	0.0055 (2)
O1	0.0269 (16)	0.0306 (17)	0.0260 (16)	0.0013 (15)	-0.0068 (13)	0.0022 (14)
N1	0.0179 (16)	0.0204 (18)	0.0182 (17)	0.0037 (15)	-0.0015 (13)	0.0042 (14)
N2	0.0286 (17)	0.0326 (19)	0.0270 (17)	0.0030 (14)	-0.003 (2)	-0.009 (2)
C2	0.0214 (19)	0.027 (3)	0.016 (2)	0.0027 (19)	0.0010 (16)	0.0020 (17)
C3	0.024 (2)	0.024 (2)	0.024 (2)	0.0070 (18)	0.0013 (16)	0.0046 (18)
C4	0.026 (2)	0.020 (2)	0.0187 (19)	0.0013 (17)	0.0017 (16)	-0.0013 (15)
C5	0.024 (2)	0.024 (2)	0.019 (2)	0.0049 (16)	-0.0004 (16)	-0.0031 (18)
C6	0.021 (2)	0.023 (2)	0.0128 (18)	0.0052 (17)	0.0003 (15)	0.0013 (15)
C7	0.0197 (19)	0.022 (2)	0.019 (2)	0.0020 (17)	-0.0003 (15)	0.0009 (17)
C8	0.023 (2)	0.029 (2)	0.0188 (18)	0.0036 (17)	0.0015 (16)	0.0010 (17)
C9	0.027 (2)	0.028 (2)	0.023 (2)	0.0004 (18)	0.0009 (17)	0.0042 (18)
C10	0.026 (2)	0.023 (2)	0.031 (3)	0.0001 (17)	0.0013 (19)	-0.0009 (18)
C11	0.033 (2)	0.028 (2)	0.026 (2)	0.001 (2)	0.0016 (19)	-0.004 (2)
C12	0.027 (2)	0.033 (3)	0.0172 (19)	-0.0010 (19)	0.0026 (16)	-0.0004 (18)
C13	0.031 (2)	0.020 (2)	0.031 (2)	0.0041 (19)	-0.0016 (19)	0.0007 (18)
C14	0.029 (2)	0.021 (2)	0.0199 (18)	0.0020 (18)	0.0007 (16)	-0.0028 (17)
C15	0.0170 (17)	0.017 (2)	0.018 (2)	0.0035 (16)	-0.0027 (15)	-0.0001 (16)
C16	0.025 (2)	0.022 (2)	0.0131 (18)	0.0017 (16)	0.0016 (15)	0.0015 (15)
C17	0.0219 (19)	0.025 (2)	0.0174 (19)	0.0030 (16)	0.0019 (15)	-0.0021 (16)
C18	0.0228 (19)	0.019 (2)	0.0196 (19)	0.0006 (16)	-0.0029 (14)	0.0030 (15)
C19	0.026 (2)	0.028 (2)	0.0150 (18)	0.0051 (18)	-0.0014 (16)	-0.0002 (17)
C20	0.028 (2)	0.027 (2)	0.014 (2)	0.0015 (17)	-0.0006 (15)	-0.0017 (15)

Geometric parameters (\AA , $^\circ$)

Br1—C18	1.944 (4)	C9—H9	0.9500
O1—C2	1.217 (6)	C10—C11	1.354 (7)
N1—C6	1.356 (6)	C10—H10	0.9500
N1—C2	1.456 (6)	C11—C12	1.436 (7)
N1—C7	1.503 (6)	C11—H11	0.9500
N2—C14	1.127 (6)	C12—H12	0.9500
C2—C3	1.485 (7)	C13—H13A	0.9800
C3—C4	1.352 (7)	C13—H13B	0.9800
C3—H3	0.9500	C13—H13C	0.9800
C4—C5	1.464 (7)	C15—C20	1.342 (6)
C4—C13	1.548 (6)	C15—C16	1.389 (6)
C5—C14	1.429 (6)	C16—C17	1.420 (6)
C5—C6	1.433 (7)	C16—H16	0.9500
C6—C15	1.520 (6)	C17—C18	1.329 (6)
C7—C8	1.353 (6)	C17—H17	0.9500

C7—C12	1.360 (6)	C18—C19	1.380 (6)
C8—C9	1.437 (7)	C19—C20	1.417 (6)
C8—H8	0.9500	C19—H19	0.9500
C9—C10	1.371 (7)	C20—H20	0.9500
C6—N1—C2	121.0 (4)	C10—C11—H11	119.1
C6—N1—C7	120.1 (4)	C12—C11—H11	119.1
C2—N1—C7	118.6 (3)	C7—C12—C11	121.1 (4)
O1—C2—N1	116.5 (4)	C7—C12—H12	119.5
O1—C2—C3	126.0 (4)	C11—C12—H12	119.5
N1—C2—C3	117.5 (4)	C4—C13—H13A	109.5
C4—C3—C2	123.2 (4)	C4—C13—H13B	109.5
C4—C3—H3	118.4	H13A—C13—H13B	109.5
C2—C3—H3	118.4	C4—C13—H13C	109.5
C3—C4—C5	115.7 (4)	H13A—C13—H13C	109.5
C3—C4—C13	121.7 (4)	H13B—C13—H13C	109.5
C5—C4—C13	122.6 (4)	N2—C14—C5	176.7 (5)
C14—C5—C6	119.2 (4)	C20—C15—C16	116.6 (4)
C14—C5—C4	117.1 (4)	C20—C15—C6	121.9 (4)
C6—C5—C4	123.6 (4)	C16—C15—C6	121.4 (4)
N1—C6—C5	118.9 (4)	C15—C16—C17	123.4 (4)
N1—C6—C15	116.8 (4)	C15—C16—H16	118.3
C5—C6—C15	124.0 (4)	C17—C16—H16	118.3
C8—C7—C12	118.1 (4)	C18—C17—C16	118.8 (4)
C8—C7—N1	118.7 (4)	C18—C17—H17	120.6
C12—C7—N1	123.1 (4)	C16—C17—H17	120.6
C7—C8—C9	120.4 (4)	C17—C18—C19	119.0 (4)
C7—C8—H8	119.8	C17—C18—Br1	118.9 (3)
C9—C8—H8	119.8	C19—C18—Br1	122.1 (3)
C10—C9—C8	122.2 (4)	C18—C19—C20	121.8 (4)
C10—C9—H9	118.9	C18—C19—H19	119.1
C8—C9—H9	118.9	C20—C19—H19	119.1
C11—C10—C9	116.4 (4)	C15—C20—C19	120.4 (4)
C11—C10—H10	121.8	C15—C20—H20	119.8
C9—C10—H10	121.8	C19—C20—H20	119.8
C10—C11—C12	121.8 (5)		
C6—N1—C2—O1	176.5 (4)	C2—N1—C7—C12	75.3 (5)
C7—N1—C2—O1	-10.1 (6)	C12—C7—C8—C9	-0.5 (6)
C6—N1—C2—C3	-4.8 (6)	N1—C7—C8—C9	177.2 (4)
C7—N1—C2—C3	168.5 (4)	C7—C8—C9—C10	0.5 (7)
O1—C2—C3—C4	-178.3 (5)	C8—C9—C10—C11	0.2 (7)
N1—C2—C3—C4	3.2 (7)	C9—C10—C11—C12	-0.9 (7)
C2—C3—C4—C5	-0.2 (7)	C8—C7—C12—C11	-0.1 (7)
C2—C3—C4—C13	178.2 (4)	N1—C7—C12—C11	-177.8 (4)
C3—C4—C5—C14	177.5 (4)	C10—C11—C12—C7	0.9 (7)
C13—C4—C5—C14	-0.8 (7)	N1—C6—C15—C20	-117.6 (5)
C3—C4—C5—C6	-1.4 (7)	C5—C6—C15—C20	68.0 (6)

C13—C4—C5—C6	−179.8 (4)	N1—C6—C15—C16	65.0 (6)
C2—N1—C6—C5	3.4 (6)	C5—C6—C15—C16	−109.5 (5)
C7—N1—C6—C5	−169.9 (4)	C20—C15—C16—C17	−0.8 (6)
C2—N1—C6—C15	−171.3 (4)	C6—C15—C16—C17	176.8 (4)
C7—N1—C6—C15	15.4 (6)	C15—C16—C17—C18	1.3 (7)
C14—C5—C6—N1	−179.1 (4)	C16—C17—C18—C19	−0.9 (7)
C4—C5—C6—N1	−0.2 (7)	C16—C17—C18—Br1	179.7 (3)
C14—C5—C6—C15	−4.8 (7)	C17—C18—C19—C20	0.1 (7)
C4—C5—C6—C15	174.1 (4)	Br1—C18—C19—C20	179.5 (3)
C6—N1—C7—C8	71.1 (5)	C16—C15—C20—C19	−0.1 (7)
C2—N1—C7—C8	−102.3 (5)	C6—C15—C20—C19	−177.6 (4)
C6—N1—C7—C12	−111.3 (5)	C18—C19—C20—C15	0.4 (7)

Hydrogen-bond geometry (Å, °)

D—H···A	D—H	H···A	D···A	D—H···A
C16—H16···N2 ⁱ	0.95	2.55	3.234 (6)	129
C17—H17···O1 ⁱⁱ	0.95	2.56	3.342 (6)	140
C20—H20···O1 ⁱⁱⁱ	0.95	2.40	3.256 (6)	150

Symmetry codes: (i) $-x+3/2, y-1/2, z-1/2$; (ii) $x+1/2, -y+1/2, z$; (iii) $-x+1, -y+1, z+1/2$.